sustainability

MDPI

Article

A Site-Specific Wind Energy Potential Analysis Based on Wind Probability Distributions: A Ciudad Juárez-México Case Study

Carlos Adrián Hernández-Meléndez [1], Luis Alberto Rodríguez-Picón [1,*], Iván Juan Carlos Pérez-Olguín [1], Felipe Adrián Vázquez-Galvez [2], Jesús Israel Hernández-Hernández [3] and Luis Carlos Méndez-González [1]

[1] Department of Industrial Engineering and Manufacturing, Institute of Engineering and Technology, Autonomous University of Ciudad Juárez, Ciudad Juárez 32310, Mexico; al182971@alumnos.uacj.mx (C.A.H.-M.); ivan.perez@uacj.mx (I.J.C.P.-O.); luis.mendez@uacj.mx (L.C.M.-G.)
[2] Department of Civil and Environmental Engineering, Institute of Engineering and Technology, Autonomous University of Ciudad Juárez, Ciudad Juárez 32310, Mexico; fvazquez@uacj.mx
[3] Department of Electrical and Computer Engineering, Institute of Engineering and Technology, Autonomous University of Ciudad Juárez, Ciudad Juárez 32310, Mexico; israel.hernandez@uacj.mx
* Correspondence: luis.picon@uacj.mx

Abstract: Wind energy production has been a relevant topic of research for several years. Specifically, the estimation of wind energy potential has received important attention in different regions of the world. One of the main considerations for these estimations is based on the modeling of wind speed data based on probability density functions (PDF), given that once the best distribution for wind speed data is determined, the wind energy potential can be estimated. The objective of this paper is to investigate the wind speed and wind energy potential in Ciudad Juárez, México. To achieve this, three meteorological stations were installed in strategic open sites at a height of 10 meters within and on the edges of the city. Speed data were recorded for each meteorological station every ten minutes over a one-year period. The wind speed data were studied to define the best-fitting distribution, and different commercial wind turbines were considered to estimate the power curves for each location. With the characterized power curves, it was possible to estimate the potential energy production. In addition, wind shear was considered to estimate the energy production with wind turbines that have greater heights. The results show the importance of selecting the best distribution to estimate the wind energy potential of certain regions where measurements can be obtained from different locations.

Keywords: mixture distributions; power curves; annual energy production; Akaike information criterion; probability density function

Citation: Hernández-Meléndez, C.A.; Rodríguez-Picón, L.A.; Pérez-Olguín, I.J.C.; Vázquez-Galvez, F.A; Hernádez-Hernández, J.I.; Méndez-González, L.C. A Site-Specific Wind Energy Potential Analysis Based on Wind Probability Distributions: A Ciudad Juárez-México Case Study. *Sustainability* **2024**, *16*, 9486. https://doi.org/10.3390/su16219486

Academic Editor: Abdul Rehman

Received: 4 September 2024
Revised: 21 October 2024
Accepted: 28 October 2024
Published: 31 October 2024

1. Introduction

Renewable energy sources have received great attention in recent decades as an alternative to mitigate environmental problems and satisfy energy needs worldwide [1]. Specifically, wind power generation has become an important option as a clean renewable energy source [2], given that it is accessible, sustainable, and environmentally friendly [3]. This is because it is an alternative to generate electricity without depending on fossil fuels, does not release emissions, and does not require water as a cooling alternative. Furthermore, many regions have adopted this energy generation alternative to drive wind turbines to satisfy energy needs [4]. Precisely, for the development of wind energy systems, it is necessary to have novel wind turbine technologies [5,6] and wind speed data of specific regions to study their characteristics and properties, which allows us to determine the energy potential [7,8].

Several models have been considered in the literature to study the statistical properties of wind speed data; in particular, probabilistic models have been specifically considered. Morgan et al. [9] mention that the PDF of wind speed data is important in determining wind energy production, the design of wind turbines, and the location of wind turbines. This

means that the selection of the PDF that best describes the wind speed data could reduce uncertainty and provide confidence and risk reduction in wind energy systems [10–12].

Specifically, the Weibull distribution has been presented as an important option to model wind speed data [13]. This is because it is a flexible distribution that can easily adapt to different behaviors [11,14–20]. The Weibull distribution has a bigger probability in the right tail, which results in flexibility in modeling wind speed data that have extreme velocities in the direction of the right tail [21,22]. Previous literature [23] mentions that the Weibull distribution is not capable of modeling all the behaviors of wind speed data in an efficient manner, which justifies the use of other PDFs to extend the systematic analysis of wind distributions to determine the wind energy potential [24–26].

Beyond the Weibull distribution, many PDFs have been considered in the literature to model wind speed data. Ouarda and Charron [27], Kollu et al. [28], Carta and Ramirez [29] studied mixtures of distributions to model wind speed data; specific mixtures of the gamma, lognormal, Weibull, Gumbel, and normal distributions have also been studied. These models are appropriate when bimodal wind speed data are present. Non-parametric models have been considered, given that they provide a good fit for wind speed data without the preposition of dealing with parameters [30], which is the case with theoretical distributions. Variations of PDFs, such as the Weibull distribution, have been considered along with artificial intelligence methods. Asghar and Liu [31] developed a methodology based on the adaptive neuro-fuzzy inference system to estimate the parameters of the Weibull distribution. Zhang et al. [32] combined artificial intelligence methods based on the fast correlation-based filter and radial basis functions for the interval estimation of wind speed. Miao et al. [33] developed an optimal score-radar map to find the best-fitting distribution for certain regions. Fadare [34] considered an artificial neural network to model the wind speed profile in Nigeria. Ouarda et al. [35] considered L-moment ratio diagrams to select the best distribution for wind speed data of a certain region. Stochastic approaches have also been presented as alternatives to fit wind speed data. Jónsdóttir and Milano [36] developed a method to model wind speed measurements based on dynamic stochastic models. Most of the previously discussed works deal with the process of fitting different PDFs or models to wind speed data; then, based on various goodness of fit tests or information criteria, the best-fitting distribution or model is defined [37–39].

Previous works have been presented in the literature that deals with finding the best PDFs for wind speed data of certain regions based on different methods [10,27,40–42]. The objective of this paper is to focus beyond this aspect and find the best PDF for the region of interest. Specifically, we estimate the power curves (PCs) considering the cumulative distribution function (CDF) of the best-fitting PDF and the production profile of different wind turbines. This is a relevant aspect as PCs allow us to determine the amount of potential energy production at certain wind speeds by considering the performance of a specific wind turbine, which is important for the selection of wind energy production locations. In this sense, we consider the characterized PCs for the locations of interest to estimate the annual energy production. Furthermore, wind shear is also considered for extrapolating the collected wind speed data at different heights to estimate wind energy production with turbines of greater capacity. These estimations complement the method to assess the wind energy production potential, which contributes to the decision-making process of developing wind farms. The region of interest is Ciudad Juárez, which is a northern city in México. The study is focused on this region, as this is an industrial city in which efforts have been made to obtain wind speed data to determine the wind energy potential. This is with the objective of adopting sustainable strategies that can provide an alternative to satisfy energy consumption needs. The proposed method can be summarized by first collecting wind speed data from three meteorological stations. Then, the best-fitting PDFs are selected via information criteria. The interaction between the wind potential given by the best-fitting PDFs and various wind turbines is evaluated based on an extension of the method proposed by [43] to obtain the PC. Given that PCs enable us to estimate the

conversion of the available wind energy transferred to wind power generators [12,44–46], we also present an estimation of the potential energy production for the region of interest.

This paper is organized as follows: in Section 2, generalities of the region of interest are presented. In Section 3, the considered methodology is presented and discussed. In Section 4, the obtained results are presented and discussed according to the proposed method. Finally, in Section 5, the conclusions are presented.

2. Generalities of the Study Region

Ciudad Juárez is a city located in northern México, in the state of Chihuahua, bordering the US city of El Paso, Texas. It is located in the middle of Chihuahua's desert, which is the largest in North America. In the summer, the daily maximum temperatures remain in a range between 35 °C and 40 °C during the day, having large oscillations between day and night of 16 °C on average [47]. The prevailing winds during the warm seasons are mostly from the east, with an annual average wind speed of 4.63 m/s [48]. Due to its climatological characteristics, this region is considered as a case study to assess the wind energy production potential. Rainfall in Ciudad Juárez is relatively low, with an annual average of 237.5 mm, according to National Meteorological Service (SMN) data from 1961–1990. The wettest months are July and August, with normal monthly precipitation values of 46 mm and 46.4 mm, respectively. Extreme rainfall events have occurred, with the highest daily rainfall reaching 113.5 mm in July 1968. This variability underscores the challenges in water resource management in a desert region heavily reliant on sporadic and intense rainfall events [47]. Three meteorological stations distributed in the region were considered to obtain meteorological data, which include wind speed, temperature, wind density, atmospheric pressure, etc. These data were obtained from the three stations known as IIT, Anapra, and Clínica at the servers from the climatology laboratory of the Universidad Autónoma de Ciudad Juárez [49]. Each station has an anemometer that collects data at a height of 15 m. It should be noted that these stations are located at different latitudes, which means that different measurements are expected to be obtained. Furthermore, the IIT station is located within the city, and the Anapra and Clínica stations are located on the outskirts of the city, which also contributes to the possible differences in the wind speed measurements. The geographical location of these stations is presented in Figure 1, while in Table 1, the description of the stations is presented.

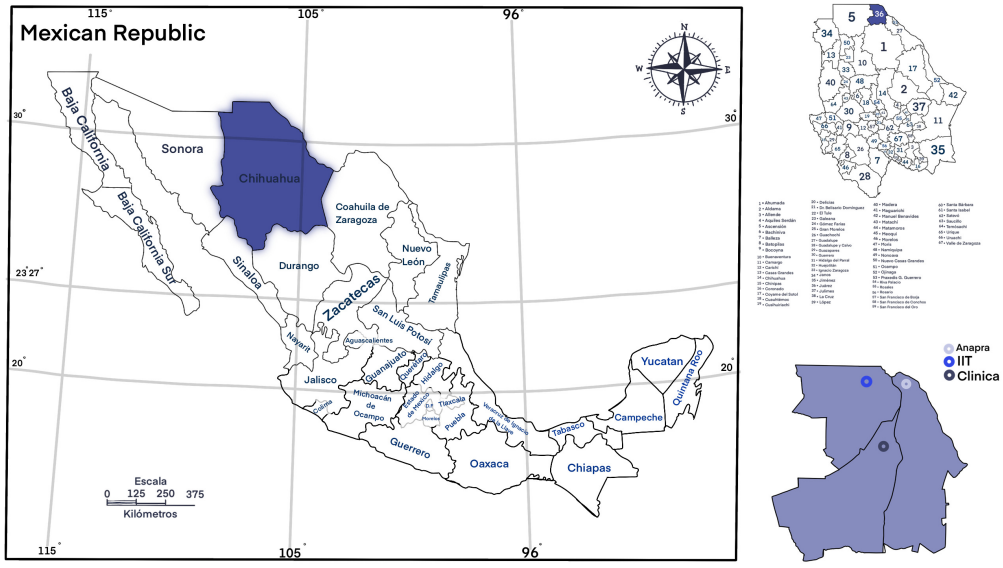

Figure 1. Location of the three meteorological stations.

Table 1. Characteristics of the three considered stations.

Station	Latitude	Longitude	Altitude	Period
Anapra	31°46′23.94″ N	106°33′51.48″ W	1218 (m)	2019/01–2019/12
Clínica	31°39′19.38″ N	106°27′59.42″ W	1212 (m)	2019/04–2019/12
IIT	31°44′34.90″ N	106°26′00.52″ W	1158 (m)	2019/01–2019/12

3. Data and Models

In this section, a description of the considered methodology is presented. In Figure 2, a flow chart that enlists the proposed steps is presented.

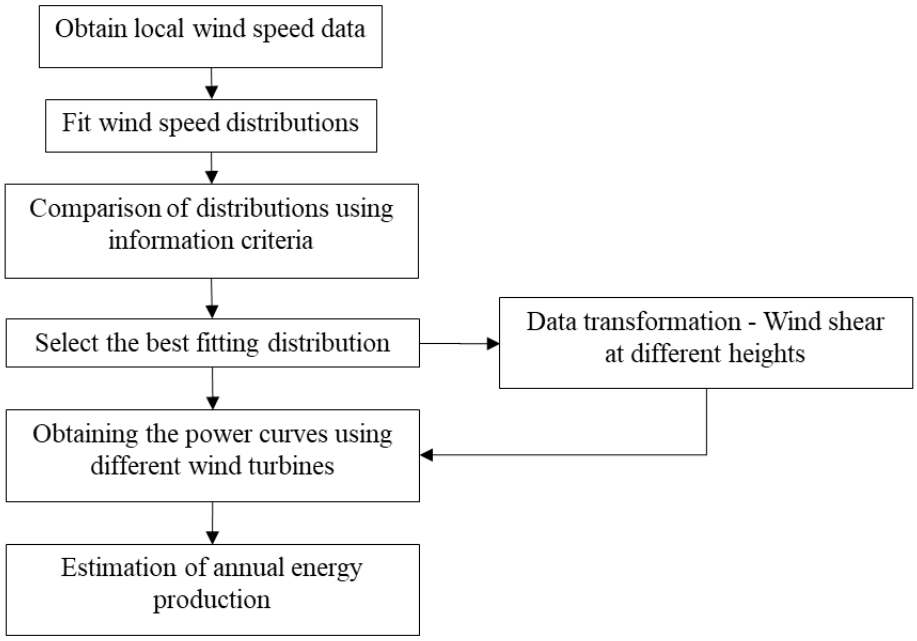

Figure 2. Flow chart of the considered method.

3.1. Obtaininig of the Local Wind Speed Data

The wind speed data were collected at one-minute intervals for the IIT station and five-minute intervals for the Anapra and Clinica stations; the data were exported and organized in Excel files. Missing values from the three stations were removed for further analysis. The data were obtained from the climatology laboratory of the Universidad Autonoma de Ciudad Juárez, available at https://erecursos.uacj.mx/communities/b27494f3-ef56-4f2b-9b58-12db83e20176 (accessed on 1 December 2023).

3.2. Fitting Probability Distributions to the Wind Speed Data

A total of 16 PDFs were considered to fit the collected wind speed data. In general, these parametric distributions are described in Table 2 and are defined as $f(x|\theta)$, where x represents a variable that represents wind speed data, and θ represents a parameter or a vector of parameters. Each distribution has different parameters, which have been defined as follows: μ represents a location parameter, m represents a threshold parameter, α is a scale parameter, k is a shape parameter, ρ is a second scale parameter, h is a second shape parameter, and ω is a mixture parameter.

Classical distributions to fit wind speed data were considered [10,15,30,40]. Moreover, we considered three distributions that are not generally used to model wind speed: the exponentiated Weibull distribution, the inverse Weibull distribution, and the inverse Gaussian distribution. The exponentiated Weibull distribution has been presented as an alternative to model lifetime data given that it has similar properties to the Weibull and gamma distributions; however, it has more flexible properties to model hazard rate func-

tions [50], which is also the case for the inverse Weibull distribution. Lastly, the inverse Gaussian distribution has been presented as an important option to model skewed data [51], which is generally the case when dealing with wind speed. All these distributions are presented in Table 2.

Table 2. Considered distributions to fit the collected wind speed data.

Distribution (Nomenclature)	PDF	Domain
Weibull–Two parameters (W2)	$f(x) = \frac{k}{\alpha}\left(\frac{x}{\alpha}\right)^{k-1} exp\left\{-\left(\frac{x}{\alpha}\right)^{k}\right\}$	$(0, \infty)$
Gamma (GA)	$f(x) = \frac{x^{k-1}}{\alpha^{k}\Gamma(k)} exp\left\{-\frac{x}{\alpha}\right\}$	$(0, \infty)$
Lognormal–Two parameters (LN2)	$f(x) = \frac{1}{x\alpha\sqrt{2\pi}} exp\left\{-\frac{(lnx-\mu)^2}{2\alpha^2}\right\}$	$(0, \infty)$
Weibull–Three parameters (W3)	$f(x) = \frac{k}{\alpha}\left(\frac{x-m}{\alpha}\right)^{k-1} exp\left\{-\left(\frac{x-m}{\alpha}\right)^{k}\right\}$	$(0, \infty)$
Lognormal–Three parameters (LN3)	$f(x) = \frac{1}{(x-m)\alpha\sqrt{2\pi}} exp\left\{-\frac{(ln(x-m)-\mu)^2}{2\alpha^2}\right\}$	$(0, \infty)$
Generalized extreme value (GEV)	$f(x) = \frac{1}{\alpha}\left[1-\frac{k}{\alpha}(x-\mu)\right]^{\frac{1}{k}-1} exp\left\{-\left[1-\frac{k}{\alpha}(x-\mu)\right]^{\frac{1}{k}}\right\}$	$(0, \infty)$
Kappa (KAP)	$f(x) = \left(\frac{k}{\alpha}\right)\left(k+\left(\frac{x}{\alpha}\right)^{k}\right)^{-\left(\frac{k+1}{k}\right)}$	$(0, \infty)$
Mixture - Two Weibull (MWW)	$f(x) = \omega\left[\frac{k_1}{\alpha_1}\left(\frac{x}{\alpha_1}\right)^{k_1-1} exp\left\{-\left(\frac{x}{\alpha_1}\right)\right\}\right] + (1-\omega)\left[\frac{k_2}{\alpha_2}\left(\frac{x}{\alpha_2}\right)^{k_2-1} exp\left\{-\left(\frac{x}{\alpha_2}\right)\right\}\right]$	$(0, \infty)$
Mixture–Two Gamma (MGG)	$f(x) = \omega\left[\frac{x^{k_1-1}}{\alpha_1^{k_1}\Gamma(k_1)} exp\left\{-\frac{x}{\alpha_1}\right\}\right] + (1-\omega)\left[\frac{x^{k_2-1}}{\alpha_2^{k_2}\Gamma(k_2)} exp\left\{-\frac{x}{\alpha_2}\right\}\right]$	$(0, \infty)$
Exponentiated Weibull (EXW)	$f(x) = \left(\frac{hk}{\alpha}\right)\left(\frac{x}{\alpha}\right)^{k-1}\left[1-exp\left\{-\left(\frac{x}{\alpha}\right)^{k}\right\}\right]^{h-1} exp\left\{-\left(\frac{x}{\alpha}\right)^{k}\right\}$	$(0, \infty)$
Inverse Weibull (INW)	$f(x) = \alpha k x^{-(x+1)} exp\left\{-\alpha x^{-k}\right\}$	$(0, \infty)$
Inverse Gaussian (IG)	$f(x) = \sqrt{\frac{k}{2\pi x^3}} exp\left\{-\frac{k(x-\mu)^2}{2\mu^2 x}\right\}$	$(0, \infty)$
Burr (BR)	$f(x) = \frac{\left[k\rho\left(\frac{x}{\alpha}\right)\right]^{k-1}}{\alpha\left[1+\left(\frac{x}{\alpha}\right)^{k}\right]^{\rho+1}}$	$(0, \infty)$
Rayleigh (RA)	$f(x) = \frac{x}{\alpha^2} exp\left\{-\frac{x^2}{2\alpha^2}\right\}$	$(0, \infty)$
Mixture–Gamma–Weibull (MGW)	$f(x) = \omega\left[\frac{x^{k_1-1}}{\alpha_1^{k_1}\Gamma(k_1)} exp\left\{-\frac{x}{\alpha_1}\right\}\right] + (1-\omega)\left[\frac{k_2}{\alpha_2}\left(\frac{x}{\alpha_2}\right)^{k_2-1} exp\left\{-\left(\frac{x}{\alpha_2}\right)\right\}\right]$	$(0, \infty)$
Mixture–Lognormal–Generalized extreme value (MLGEV)	$\omega\left[\frac{1}{x\alpha_1\sqrt{2\pi}} exp\left\{-\frac{(lnx-\mu_1)^2}{2\alpha_1^2}\right\}\right] + (1-\omega)\left[\frac{1}{\alpha_2}\left[1-\frac{k}{\alpha_2}(x-\mu_2)\right]^{\frac{1}{k}-1} exp\left\{-\left[1-\frac{k}{\alpha_2}(x-\mu_2)\right]^{\frac{1}{k}}\right\}\right]$	$(0, \infty)$

On the other hand, mixture distributions have been presented as an important option to model bimodal data; these PDFs are constructed considering linear combinations of two or more distributions [27] and have the next parametric form for two components:

$$f(x|\omega, \theta_1, \theta_2) = \omega f_1(x|\theta_1) + (1-\omega) f_2(x|\theta_2), \quad (1)$$

where ω is the mixture parameter, θ_1 and θ_2 are parameters or vectors of parameters for individual PDFs, and f_1 and f_2 represent the parametric form of individual PDFs. These parametric models have important advantages given that they can present a better fit for wind speed data compared to one-component distributions [27,52].

For any parametric distribution $f(x_i|\theta)$, wind speed data are considered to fit the models based on different methods. First, we discuss the maximum likelihood estimation (MLE). Considering independent and identically distributed random samples $i = 1, 2, \ldots, n$, the parameters (or vector of parameters) θ are estimated by maximizing the likelihood function $L(\theta|x_i)$, which is defined as follows:

$$L(\theta|x_i) = \prod_{i=1}^{n} f(x_i|\theta). \quad (2)$$

Such a likelihood function can be solved by considering different optimization routines that are included in the *R v4.3.2* statistical software. In this paper, the *"fitdistrplus"* package [53] is specifically used to solve the function in (2) for any of the PDFs in Table 2.

The maximum goodness-of-fit estimation (MGE) method is also considered to estimate certain distributions (mixture distributions); this method considers a random sample $x_1, x_2, \ldots, x_n$ with a cumulative distribution function (CDF) defined as $F(x)$, order statistics defined as $x_{(1)} \leq x_{(2)} \ldots \leq x_{(n)}$, and finally, an empirical distribution function defined as $S_n(x)$. Then, the estimation of parameters is carried out by numerically minimizing the distance between $F(x)$ and $S_n(x)$. There are different distance measures that can be considered to account for the difference between $F(x)$ and $S_n(x)$, such as the Kolmogorov–Smirnov (KS), Cramer–von Mises (CVM), and Anderson–Darling (AD) methods; all of these are considered in the *fitdistrplus* package. Finally, the moment-matching estimation

(MME) method is also considered for estimating the mixture distribution in this paper. This method consists of finding values of the parameters of interest that match the values between the theoretical and sample moments obtained from the data. It is well known that this method presents consistent estimations. However, it is usually considered to obtain initial guesses to initiate the MLE estimation method. In this paper, it is considered to estimate the parameters of the mixture distribution between the lognormal and generalized extreme value distributions, as this is a complex function that cannot be directly solved via MLE.

3.3. Comparison of Distributions and Selecting the Best via Information Criteria

There are several statistics to assess the goodness-of-fit among different distributions fitted to certain data. Distance statistics such as those considered in the MGE method (KS, CVM, and AD), the chi-squared test, and the R^2 coefficient are normally considered to select the best-fitting PDF [10,27,30,42]. However, the R^2 coefficient does not account for assessing the goodness-of-fit of a model [54]. Furthermore, the goodness-of-fit tests do not account for the complexity of the studied models. On the other hand, although the AD test may be a more powerful test compared to the KS test, it is complex to use when fitting different distributions to the same dataset, given that it considers the specific distribution to compute the critical values.

Information criteria are important statistical measures that account for quantifying the performance of a certain model to explain sampled data by considering the complexity of the model. Specifically, the Akaike information criterion (AIC) considers the Kullback–Leibler divergence to account for the distance between a true model and a candidate model. This criterion considers the linearized version of the likelihood function in (2), also known as the log-likelihood function and defined as $l(\theta|x_i) = log(L(\theta|x_i))$. The log-likelihood reflects the goodness-of-fit of the fitted PDF $f(x_i|\theta)$ to the data x_i [39]. The AIC is defined as follows:

$$AIC = -2l(\theta|x_i) + 2k, \tag{3}$$

where k represents the number of parameters of the candidate model. The term $2k$ represents a bias correction. Generally, the model that is the closest to the true generating model will result in the smallest AIC value. In this paper, we consider the AIC to select the best-fitting distribution for the collected wind speed data from the three stations.

3.4. Obtaining of the Power Curves

PCs represent the available wind energy conversion transferred by the wind turbines. This accounts for the relationship between the wind speed and the generated power that the wind turbine with a certain height can transform. The PC of a wind turbine is obtained from wind speed measurements from the field by also considering measurements from environmental variables. However, these last measurements are generally averaged and normalized to a certain wind density. The PCs for different wind turbines are usually available from manufacturers and they can be used to analyze the wind energy potential [55].

In this paper, we consider the approach proposed by Bokde et al. [43] for the characterization of wind turbine PCs, which are based on the CDF of the Weibull distribution and relates such functions with the profile of PCs provided by manufacturers. In general, a CDF is defined as follows:

$$F(x|\theta) = \int_{-\infty}^{x} f_X(t)dt. \tag{4}$$

In the case of the approach proposed by [43], the CDF of the Weibull distribution with scale parameter α and shape parameter k is defined as follows:

$$F(x) = 1 - e^{-\left(\frac{x}{\alpha}\right)^k}.$$

Then, the power (P) generated by a wind turbine as a function of the wind speed at a certain hub height is proposed to be defined as follows:

$$P = P_{max} \cdot \left(1 - e^{-\left(\frac{x}{\alpha}\right)^k}\right), \tag{5}$$

where P_{max} is the maximum power of the wind turbine. Bokde et al. [43] then proceeded to linearize the function in (5) with normalized values of P, which directly relates the power of the turbine with the CDF of the Weibull distribution. Based on this approach, in this paper, we consider extending the proposed scheme for other distributions of CDFs beyond the Weibull distribution. As it is intended to fit several distributions for the collected wind speed data, and the best-fitting PDF may result in a distribution different than the Weibull, we propose to consider the following:

$$P = P_{max} \cdot (F(x|\theta)), \tag{6}$$

where $F(x|\theta)$ is the CDF of the best-fitting distribution for the studied wind speed data. Furthermore, the power profiles from different wind turbines are considered from the database from https://www.thewindpower.net/store_manufacturer_turbine_en.php?id_type=7 (accessed on 1 January 2023).

3.5. Wind Shear of Collected Wind Speed

The wind shear refers to the wind speed variation at different heights of measurement. As the profile of the wind speed tends to be lower as the measuring height also tends to be lower, this concept results in great importance given the impact this has on the availability of power potential of a certain wind turbine. Thus, the wind speed data collected at a certain height can be extrapolated to assess the energy production for a wind turbine that may have a greater height.

According to [46], based on the log law, the wind speed v at a certain height z can be estimated as a function of the height of interest z and the surface roughness length z_0, which is a parameter that characterizes the shear and the height above the ground level where wind speed is theoretically zero. The log law is defined as follows:

$$v(z) = v(z_r)\left(\frac{ln\left(\frac{z}{z_0}\right)}{ln\left(\frac{z_r}{z_0}\right)}\right), \tag{7}$$

where $v(z_r)$ is the wind speed at a height of reference z_r. Indeed, surface roughness length may vary depending of the region of interest. Ref. [56] provides a reference table for the determination of the surface roughness length based on different types of terrains.

In this paper, as the collected wind speed is intended to be used to assess the potential energy production for wind turbines with greater heights, we considered the log law model in (7) to extrapolate the wind speed with the aim of obtaining the corresponding PC and the energy production based on different wind turbine models.

3.6. Estimation of the Annual Energy Production Based on Wind Data

The estimated energy production of a wind turbine during a time period Δt is defined as follows [46]:

$$E(\Delta t) = \int_{t_0}^{t_{0+\Delta t}} P(x(t)) \cdot \frac{\rho(t)}{1.2215}\delta(t)dt, \tag{8}$$

where $\rho(t)$ represents the air density at time t, which in this case was obtained based on the surface air pressure and the air temperature, which were monitored at climatological stations. Meanwhile, t_0 represents an initial time of interest to begin the determination of energy production. $\delta(t)$ is the Kronecker function, for which $\delta(t) = 1$ when the wind turbine is operating and $\delta(t) = 0$ when the turbine is down.

4. Results

In this section, the results obtained from the implementation of the method described in Figure 2 are presented. Firstly, a descriptive analysis was performed based on the three datasets. In Table 3, the minimum, first quartile, median, mean, third quartile, maximum, standard deviation, and variance are presented for the three stations. From this table, it can be noted that the mean speed from the stations in Anapra and Clínica is greater than the mean speed from the IIT station. This is because Anapra and Clínica are located on the outskirts of the city, while the IIT station is near the urban area. On the other hand, the skewness coefficients were obtained as 0.9158, 1.0272, and 1.3464 for the Anapra, Clínica, and IIT stations, respectively. This allows us to deduce that the distributions of the wind speed are right-skewed. Moreover, the coefficients of variation were obtained as 0.8831, 0.6786, and 0.6539, which indicate a relatively low dispersion of data.

Table 3. Descriptive statistics of the wind speed data for the three stations.

Station	Minimum	First Quartile	Median	Mean	Third Quartile	Maximum	Standard Deviation	Variance
Anapra	0	2.142	6.267	7.735	11.724	47.287	6.831	46.675
Clńica	0	4.157	7.396	8.511	12.014	42.750	5.776	33.362
IIT	0.024	1.101	1.845	2.147	2.851	15.570	1.404	1.973

Furthermore, to complement the descriptive analysis, the box plots and time series plots of the wind speed for the three stations are presented in Figure 3. It can be noted that greater wind speeds were recorded from the Clínica and Anapra stations every month. In fact, the altitude of these two stations was greater than that of the IIT station, as can be noted in Table 1.

Wind rose diagrams are also presented in Figure 4, with the aim of graphically showing the direction and duration of the wind for the three stations. From this figure, it is noted that for Anapra, the wind blew from the west around 12.5% of the time, although winds from the northwest and east were also dominant 10% of the time. Wind speed was uniform from 4 to 16 m/s. For the Clínica station, wind blew from the west, northwest, and southwest. The dominant wind speed had a range from 4 to 16 m/s. Meanwhile, for the IIT station, the wind blew mostly from the west, with velocities ranging mostly from 0 to 8 m/s.

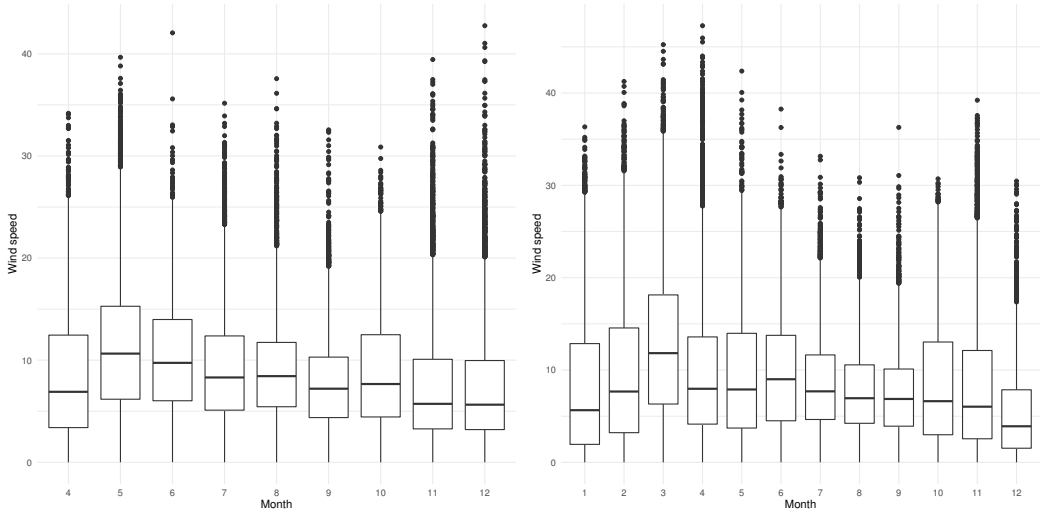

(**a**) (**b**)

Figure 3. *Cont.*

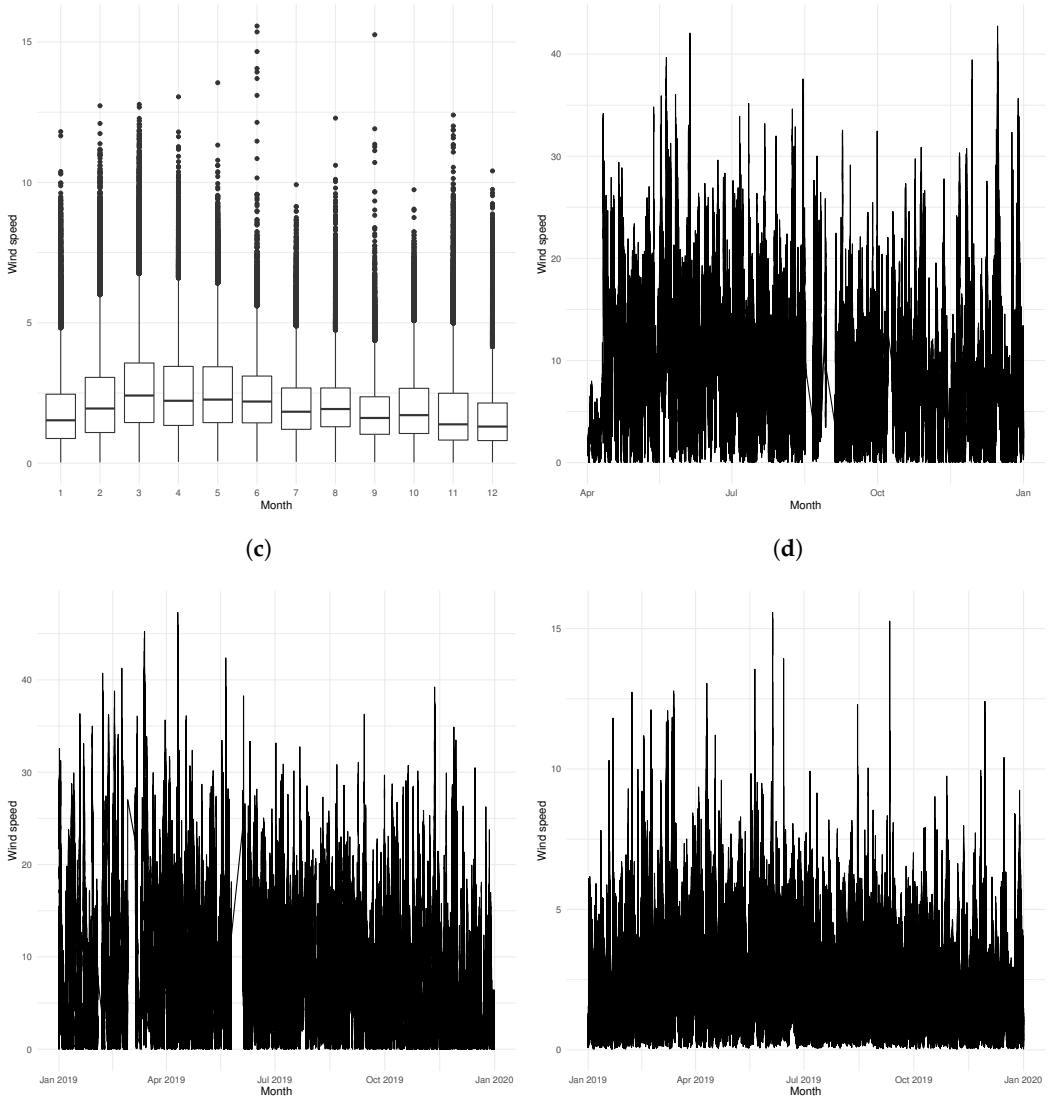

Figure 3. Graphical descriptive analysis for the wind speed of the three stations. (**a**) Box plot for the Clínica station. (**b**) Box plot for the Anapra station. (**c**) Box plot for the IIT station. (**d**) Time series plot for the Clínica station. (**e**) Time series plot for the Anapra station. (**f**) Time series plot for the IIT station.

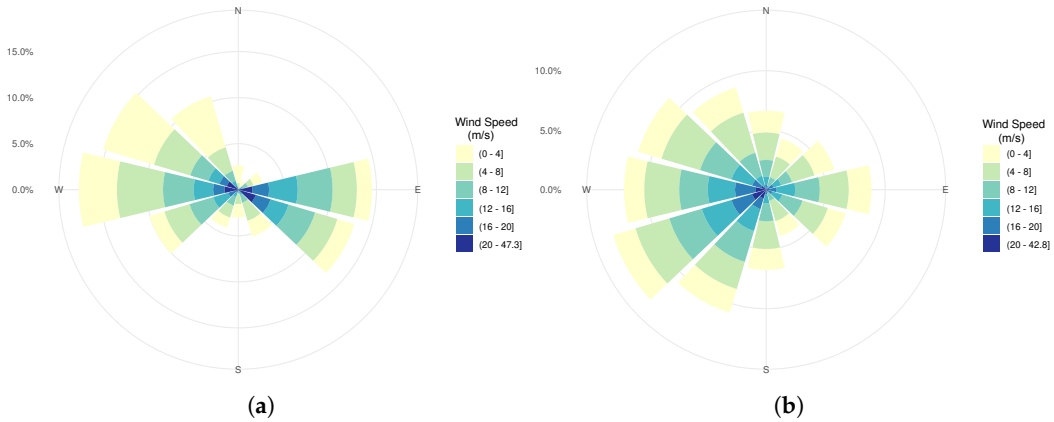

Figure 4. *Cont*.

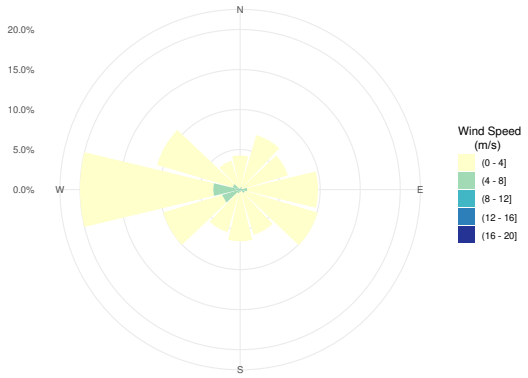

(**c**)

Figure 4. Wind rose diagrams for the wind speed of the three stations. (**a**) Wind rose for the Anapra station. (**b**) Wind rose for the Clínica station. (**c**) Wind rose for the IIT station.

4.1. Fitting the Considered Distributions to the Wind Data

The PDFs described in Table 2 were considered to fit the collected wind speed data from the three stations. For this, the *fitdistrplus* [53] package from the *R* software was used to estimate the respective parameters from every distribution. The methods considered were MLE, MME, and MGE. Fortunately, this *R* package integrates these estimation methods. Furthermore, it has the flexibility to declare distributions that are not standard in the package itself, such as the mixture distributions, i.e., gamma–gamma, Weibull–Weibull, and log-normal–generalized extreme values. In Table 4, the estimated parameters for the different distributions and the three stations are presented. These estimations are presented with the aim of characterizing the CDF for the best-fitting distribution, which will define the PC under certain determined wind turbines.

Table 4. Estimated parameters for the considered distributions in the three stations.

$f(x)$/Method	Parameters	Stations		
		Clínica	**Anapra**	**IIT**
W2/MLE	k	1.217899	0.494688	1.619208
	α	8.927912	5.783119	2.406999
RA/MLE	α	7.273111	7.297361	1.814012
G/MLE	k	1.102227	0.356256	2.405558
	α	7.723557	21.71181	0.892315
IG/MGE	k	9.497295	10.17459	2.277247
	μ	13.34213	5.612269	3.997255
BR/MLE	k	8.756322	2.911708	3.494612
	ρ	1.297835	0.546432	1.922758
	α	45.03091	28.63966	4.098941
LN2/MLE	μ	1.623222	0.164076	0.54185
	α	2.116819	4.72791	0.708024
LN3/MLE	μ	0.436431	0.820372	0.539561
	α	2.489861	1.951302	0.793198
	m	−4.72813	−1.72729	−0.40218
KAP/MLE	k	5.220631	3.275603	4.765368
	α	11.14205	8.991769	2.614413
W3/MGE	k	1.569652	1.297424	1.398526
	α	10.01682	10.30357	2.060296
	m	−0.44739	−1.59993	0.257129

Table 4. *Cont.*

$f(x)$/Method	Parameters	Stations		
		Clínica	**Anapra**	**IIT**
EXW/MLE	k	2.205107	2.009939	1.043684
	α	14.30428	16.36893	1.32843
	h	0.396761	0.199628	2.453489
MWW/MGE	k_1	4.147646	0.721678	1.420073
	α_1	2.889376	3.508384	2.168363
	k_2	1.396439	0.914911	1.454326
	α_2	9.238495	1.996823	0.396516
	w	−0.04263	2.742655	1.102644
MGG/MGE	k_1	1.194281	0.698939	2.123455
	α_1	0.194875	0.115786	1.306952
	k_2	1.400363	1.590897	2.353728
	α_2	0.400417	0.745861	1.094218
	w	1.983207	1.546984	0.022201
INW/MLE	k	0.213576	0.145404	1.223098
	α	1.219106	0.064616	1.188139
MGW/MGE	k_1	0.939225	1.100655	2.366214
	α_1	0.414885	0.542622	1.105692
	k_2	0.837682	0.74234	15.46061
	α_2	4.070996	4.419968	2.293967
	w	−1.9552	−0.94851	1.006446
MLGEV–MME	α_1	2.086203	1.41149	1.480231
	μ_1	1.545264	0.585903	0.511413
	α_2	1.988339	1.63896	0.602557
	k	0.799103	1.036238	0.742536
	μ_2	7.298414	−9.5015	−26.01969
	w	−0.02659	0.056148	−0.0296
GEV/MGE	α	429,477,537	325,605,079	1,179,839,063
	k	1,274,956,183	807,641,311	1,264,925,534
	μ	−720,191,897	−511,774,320	−474,293,383

In Table 5, the computed AIC values for all the distributions and the three stations are presented. The AIC values are ordered from lowest to largest for every station. It can be noted that for the Anapra station, the best-fitting distribution was the exponentiated Weibull (AIC = 731,684.2), and the distribution with the poorest performance was the generalized extreme value (AIC = 6,559,969). For the Clínica station, the best-fitting distribution was the gamma–Weibull mixture, which had the lowest AIC value (505,705.6); the distribution with the largest AIC was also the generalized extreme value distribution (AIC = 3,606,003). Lastly, for the IIT station, the best-fitting distribution was the exponentiated Weibull (AIC = 1,805,736), and the generalized extreme value distribution was the one with the largest AIC value (22,690,113). It should be noted that some AIC values are not reported as the obtained values tend to be infinity.

Furthermore, histograms of the wind speed from the three stations are presented in Figure 5. Moreover, the estimated distributions are superimposed with the aim of illustrating how each of these fits the data. In Figure 6, the best-fitting distributions are also presented with the aim of showing how the data from each station are well-modeled by the identified best PDF.

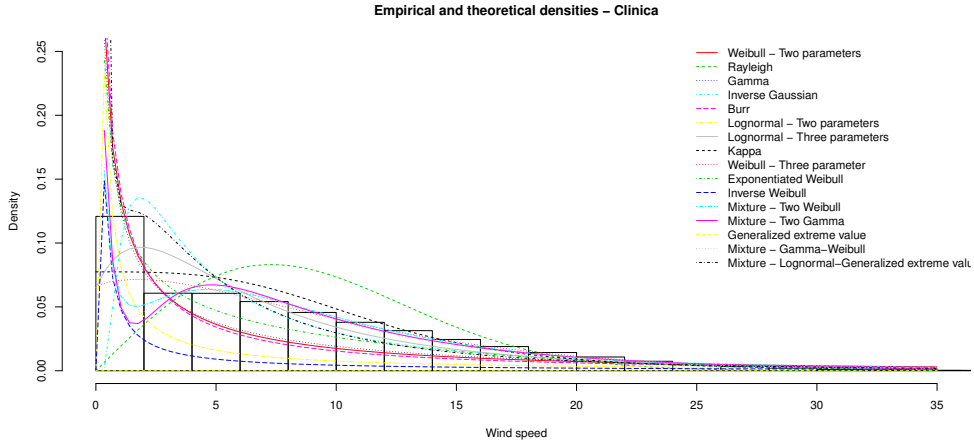

(**a**)

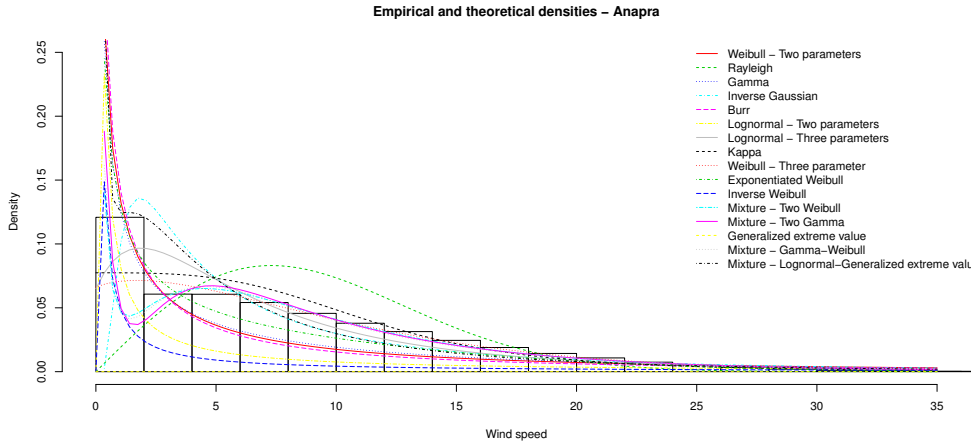

(**b**)

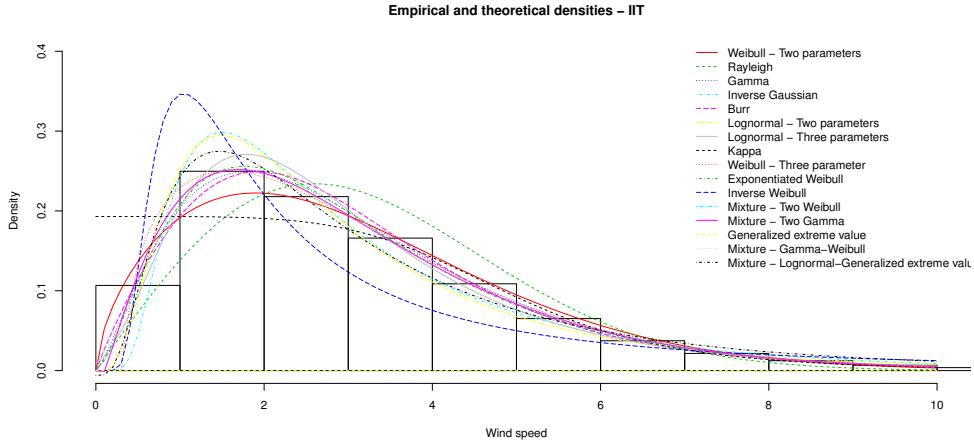

(**c**)

Figure 5. Histograms with fitted distribution curves for the wind speed of the three stations. (**a**) Histogram with all the fitted distributions for the Clínica station. (**b**) Histogram with all the fitted distributions for the Anapra station. (**c**) Histogram with all the fitted distributions for the IIT station.

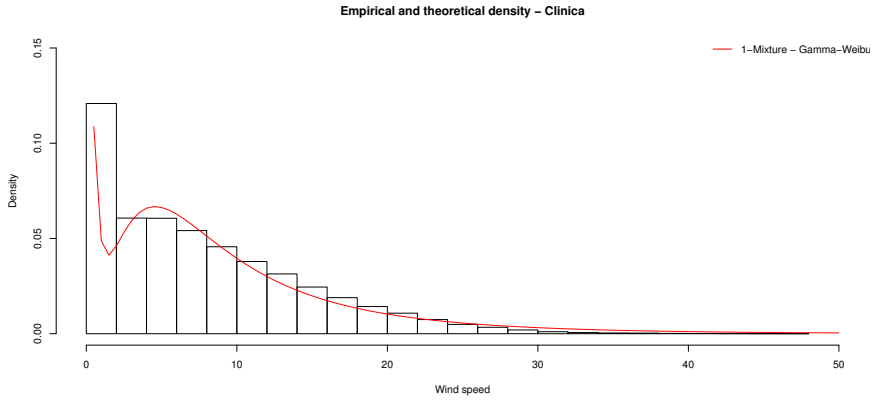

(**a**)

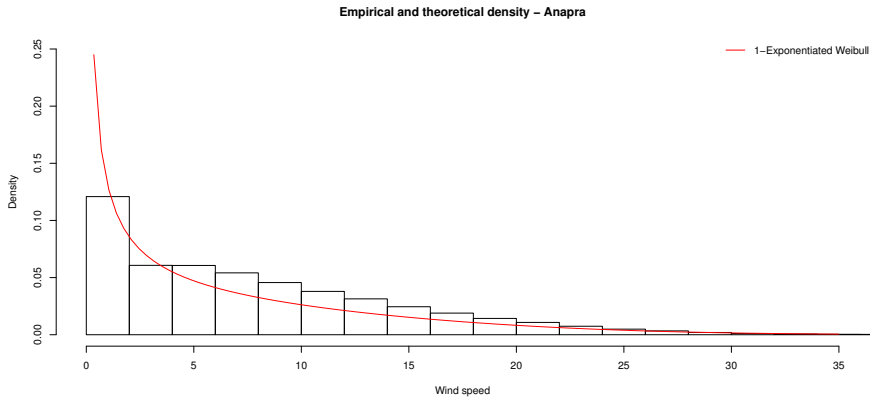

(**b**)

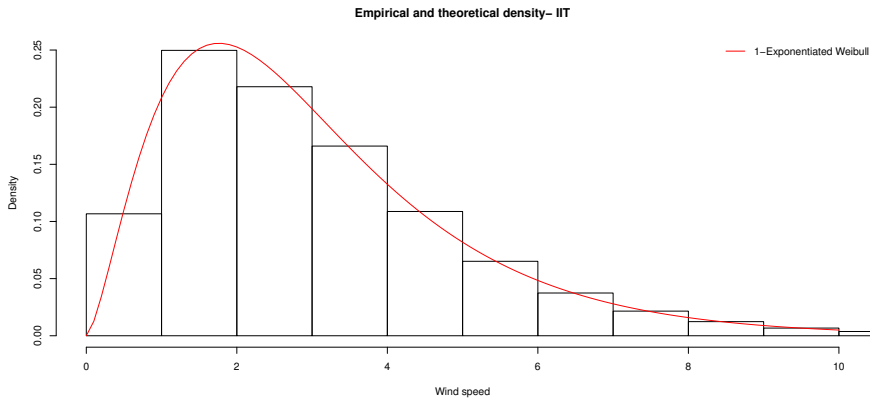

(**c**)

Figure 6. Histograms with the best-fitting distributions for each station. (**a**) Best-fitting distribution for the Clínica station. (**b**) Best-fitting distribution for the Anapra station. (**c**) Best-fitting distribution for the IIT station.

Table 5. Estimated AIC values for the fitted distributions (*AICs* that tend to infinity denoted as *).

Anapra		**Clínica**		**IIT**	
EXW	731,684.2	MGW	505,705.6	EXW	1,805,736
GA	758,407.3	EXW	510,418.8	MWW	1,806,030
MGG	794,922.1	KAP	511,954.8	GA	1,806,292
MWW	795,816.1	W3	513,285.3	MGW	1,806,460
MGW	796,863.8	MGG	513,762.3	MGG	1,806,553
W2	813,733.6	LN3	516,781	BR	1,810,058

Table 5. *Cont.*

Anapra		Clínica		IIT	
BR	848,374.4	W2	522,830.8	LN3	1,811,699
KAP	942,481.6	MWW	524,600.9	W2	1,822,666
MLGEV	958,160.6	BR	526,354.7	LN2	1,834,905
LN2	961,192.3	GA	526,644.4	RA	1,873,079
W3	968,518	RA	561,282	KAP	1,876,661
LN3	972,511.7	LN2	636,387.2	IG	1,892,098
INW	1,067,422	INW	751,179.1	INW	2,035,818
RA	1,475,097	GEV	3,606,003	MLGEV	8,556,694
GEV	6,559,969	IG	*	GEV	22,690,113
IG	*	MLGEV	*	W3	*

4.2. Characterization of the Power Curves and the Estimated Energy Production

Based on the best-fitting distributions for the three stations, the PCs can be obtained based on their respective CDFs, as discussed in Section 3.4. In the case of the Clínica station, the best-fitting distribution was the gamma–Weibull mixture, while for the Anapra and IIT stations, the exponentiated Weibull was the best-fitting distribution. The CDFs of these distributions are defined as follows:

$$F(x) = \omega\left[\frac{\Gamma(k_1, x/\alpha_1)}{\Gamma(k_1)}\right] + (1+\omega)\left[1 - exp\left\{-\left(\frac{x}{\alpha_2}\right)^{k_2}\right\}\right], \quad (9)$$

$$F(x) = \left[1 - exp\left\{-\left(\frac{x}{\alpha}\right)^{k}\right\}\right]^{h}. \quad (10)$$

The considered wind turbines for the three stations are presented in Table 6. These turbines have tower heights of 15 m, which are the same as the measurement height from the stations. The C&F Green Energy CF11 turbine has a maximum power of 11.1, while the C&F Energy CF15e turbine has a maximum power of 15.2. With this information, it is possible to characterize PCs based on the CDFs that explain the behavior of the wind speed from the three locations and the three wind turbines considered.

Table 6. Considered wind turbines at stations measuring a certain height.

Wind Turbine	Maximum Power (kw)	Rotor Diameter (m)	Tower Height (m)
C&F Green Energy CF11 9 m 11 kW	11.1	9	15
C&F Energy CF15e 13.1 m 15 kW	15.2	13.1	15

The obtained PCs, based on the CDFs in (9) and (10) and the maximum power in Table 6 from the two wind turbines, are presented in Figure 7.

These characterized PCs were used to estimate energy production. For this, the function defined in Section 3.6 was considered. In this case, the estimated power under the two scenarios of the two turbines was considered as $P(x(t))$ with the aim of estimating the corresponding energy production. The obtained results are reported in Tables 7–9 for each station.

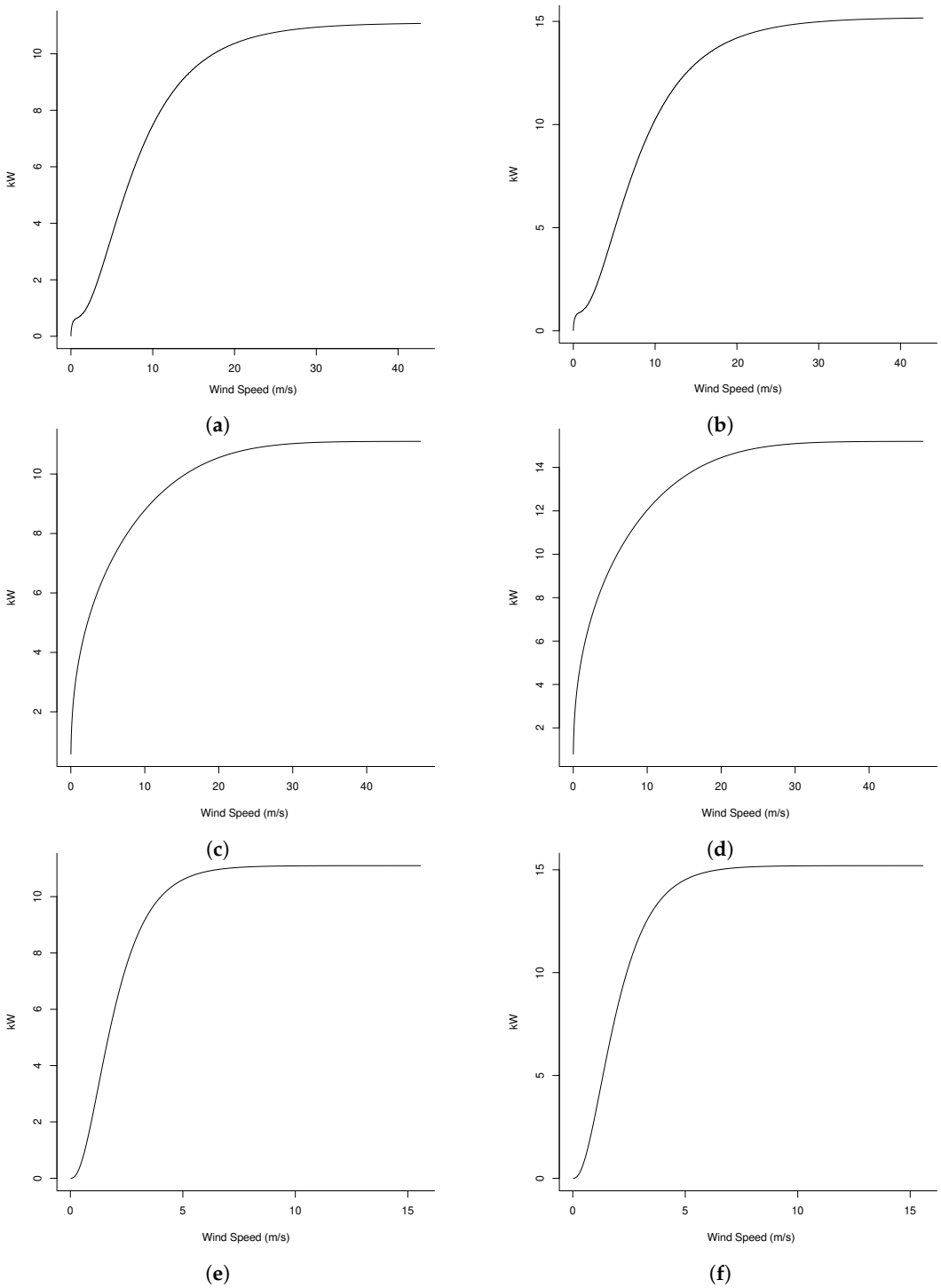

Figure 7. Characterized power curves for the three stations. (**a**) Power curve for the Clínica station–C&F Green Energy CF11. (**b**) Power curve for the Clínica station–C&F Energy CF15e. (**c**) Power curve for the Anapra station–C&F Green Energy CF11. (**d**) Power curve for the Anapra station–C&F Energy CF15e. (**e**) Power curve for the IIT station–C&F Green Energy CF11. (**f**) Power curve for the IIT station–C&F Energy CF15e.

Table 7. Estimated annual energy production in MWh for the Clínica station based on the two considered wind turbines.

Month	Mean Wind Speed (m/s)	MWh	
		C&F-Green Energy CF11	C&F-Energy CF15e
4	8.3	3.8	5.2
5	11.2	5.1	7
6	10.3	4.8	6.6
7	9.2	4.4	6
8	9.2	3.1	4.3
9	7.7	3.4	4.6
10	8.8	3.9	5.4
11	7.4	3.2	4.4
12	7.2	3.4	4.7
Annual energy production (MWh)		35.2	48.2

Table 8. Estimated annual energy production in MWh for the Anapra station based on the two considered wind turbines.

Month	Mean Wind Speed (m/s)	MWh	
		C&F Green Energy CF11	C&F Energy CF15e
1	8.3	2.1	2.9
2	9.7	1.7	2.3
3	12.7	1.9	2.6
4	9.7	2.4	3.3
5	9.5	1.9	2.6
6	9.6	2	2.8
7	8.5	2.5	3.4
8	7.7	2.3	3.1
9	7.3	2.2	3
10	8.4	2.4	3.3
11	8.2	2.1	2.9
12	5.3	1.7	2.3
Annual energy production (MWh)		25.1	34.4

Table 9. Estimated annual energy production in MWh for the IIT station based on the two considered wind turbines.

Month	Mean Wind Speed (m/s)	MWh	
		C&F Green Energy CF11	C&F Energy CF15e
1	1.8	2.63	3.6
2	2.3	2.7	3.69
3	2.7	3.33	4.56
4	2.6	3.15	4.31
5	2.6	3.33	4.57
6	2.4	3.23	4.42
7	2.1	3.06	4.19
8	2.1	3.17	4.35
9	1.8	2.7	3.69
10	2	2.88	3.94
11	1.8	2.42	3.31
12	1.6	2.39	3.28
Annual energy production (MWh)		34.99	47.91

4.3. Assessing Wind Energy Production at Different Heights

With the aim of assessing the energy production at greater heights, it was considered to extrapolate the collected data based on the log law presented in Section 3.5. The objective of this extrapolation was to study the potential energy production with higher wind turbines, given that the wind turbines studied in the previous section were only selected because they have the same height of measurement. In this case, the first considered wind turbine was Endurance X33, with the following characteristics: maximum power of 230 kW, a rotor diameter of 33.1 m,

and a tower height of 40.2 m. The second wind turbine was Suzlon S88/2100, with a maximum power of 2100 kW, a rotor diameter of 88 m, and a tower height of 79 m.

Thus, the collected wind speed data were extrapolated based on the log law in (7), with $z_r = 15$, $z_1 = 40.2$, and $z_2 = 79$ for the Endurance X33 and Suzlon S88/2100 wind turbines, respectively. Furthermore, it was considered that $z_0 = 1500$ for the Clínica, Anapra, and IIT stations, respectively, which is the corresponding value for suburbs. It should be noted that this value of z_0 was defined based on the reference table given by [56], considering the characteristics of the regions where the meteorological stations were located. The two sets of extrapolated data defined as $v(z_1)$ and $v(z_2)$ were then studied based on the flow chart from Figure 2. First, the distributions from Table 2 were fitted, and the best PDF was selected based on information criteria for every station. Then, PCs were characterized based on the CDFs of the best-fitting distributions and the power profiles from each wind turbine. Finally, the annual energy production was estimated based on the respective PCs.

For the Anapra station, it was found that the best PDF for $v(z_1)$ was the exponentiated Weibull with an $AIC = 60,1573.9$ and estimated parameters $(k = 2.2054, \alpha = 24.5573, h = 0.3969)$. Meanwhile, for $v(z_2)$, the mixture gamma–gamma resulted in the lowest AIC, 812,434.1, and estimated parameters $(k_1 = 1.6508, \alpha_1 = 0.1021, k_2 = 0.0961, \alpha_2 = 1.4096, \omega = 0.8493)$. In the case of the Clínica station, the best distributions were the mixture Weibull–Weibull and the exponentiated Weibull with AIC values of 567,645.3 and 601,573.9 and estimated parameters of $(k_1 = 0.9425, \alpha_1 = 3.1661, k_2 = 0.8210, \alpha_2 = 5.6404, \omega = -2.1187)$ and $(k = 2.1296, \alpha = 26.3512, h = 0.1853)$ for $v(z_1)$ and $v(z_2)$, respectively. Lastly, for the IIT station, the exponentiated Weibull distribution resulted in the lowest AIC value for both turbines with AIC values of 2210484 and 2422697, and estimated parameters of $(k = 1.0441, \alpha = 1.8995, h = 2.4489)$ and $(k = 1.0435, \alpha = 2.2869, h = 2.4532)$ for $v(z_1)$ and $v(z_2)$, respectively. In Figure 8, the histograms for the extrapolated data, along with the best-fitting distributions, are presented.

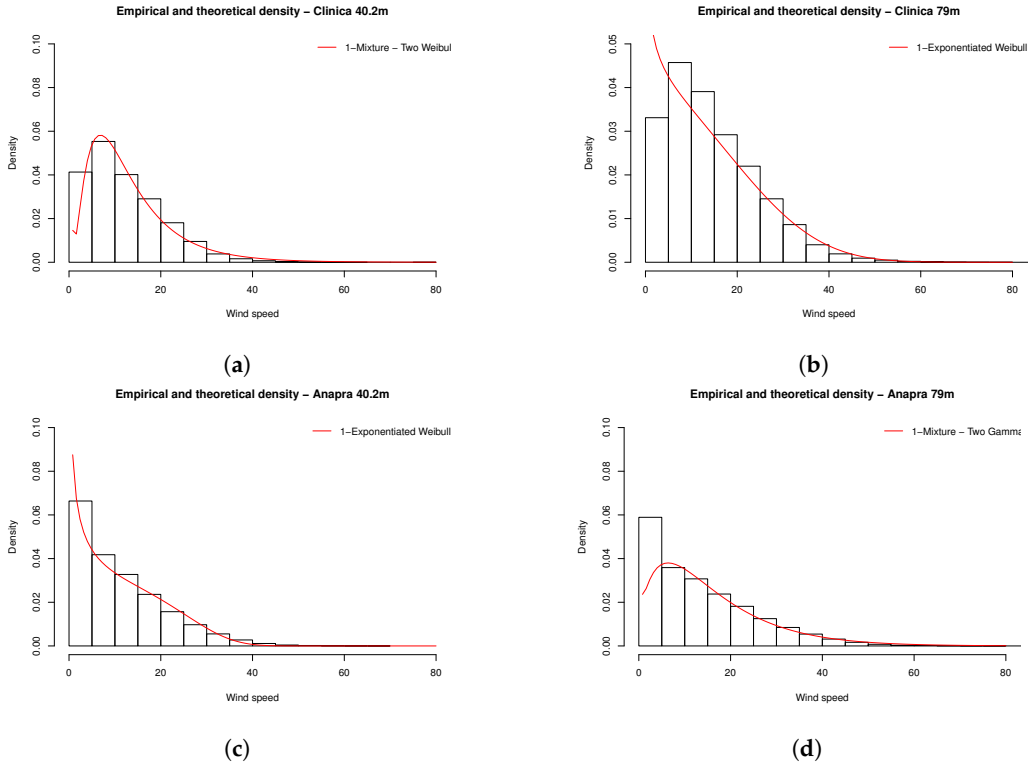

Figure 8. *Cont.*

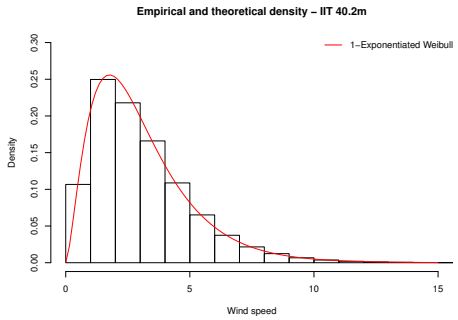

(**e**)

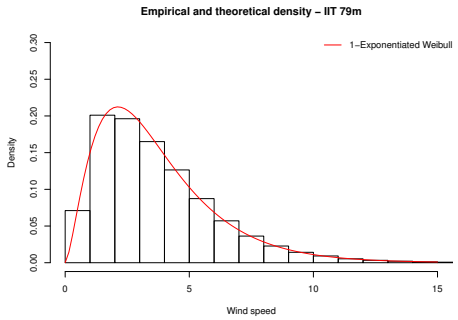

(**f**)

Figure 8. Best-fitting distributions for the considered wind turbines at the three stations. (**a**) Best-fitting distribution for the Clínica station–Endurance X33. (**b**) Best-fitting distribution for the Clínica station–Suzlon S88/2100. (**c**) Best-fitting distribution for the Anapra station–Endurance X33. (**d**) Best-fitting distribution for the Anapra station–Suzlon S88/2100. (**e**) Best-fitting distribution for the IIT station–Endurance X33. (**f**) Best-fitting distribution for the IIT station–Suzlon S88/2100.

Once the best-fitting distributions for the extrapolated data were identified, the PCs could be characterized based on the CDFs of these distributions and the power profile from each wind turbine. Again, the power profiles were obtained from the database mentioned in section 3.4 On the other hand, the CDF of the exponentiated Weibull distribution was defined in (10), while the CDFs of the gamma–gamma and Weibull-Weibull mixtures are as follows:

$$F(x) = \omega\left[\frac{\Gamma(k_1, x/\alpha_1)}{\Gamma(k_1)}\right] + (1+\omega)\left[\frac{\Gamma(k_2, x/\alpha_2)}{\Gamma(k_2)}\right], \tag{11}$$

$$F(x) = \omega\left[1 - exp\left\{-\left(\frac{x}{\alpha_1}\right)^{k_1}\right\}\right] + (1-\omega)\left[1 - exp\left\{-\left(\frac{x}{\alpha_2}\right)^{k_2}\right\}\right]. \tag{12}$$

These CDFs, along with the power profiles for each wind turbine, characterize the PCs presented in Figure 9. On the other hand, these characterized PCs are used to estimate the corresponding annual energy production based on the model presented in Section 3.6, and the results obtained are as follows. For the Clínica station with the Endurance X33 wind turbine, the estimated annual energy production was 725.2 Mwh, while for the Suzlon S88/2100, it was 3320 Mwh. For the Anapra station, the estimated annual energy production was 371.9 Mwh and 8364.4 Mwh for the Endurance X33 and Suzlon S88/2100 turbines, respectively. Lastly, the estimated annual energy production for the IIT station was 724.3 Mwh for the Endurance X33 turbine and 6619.1 Mwh for the Suzlon S88/2100 turbine.

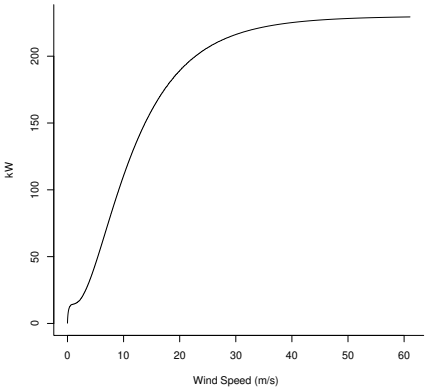

(**a**)

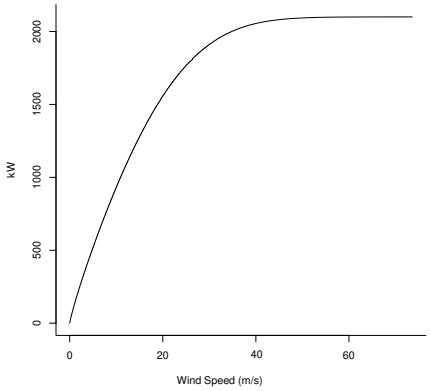

(**b**)

Figure 9. *Cont.*

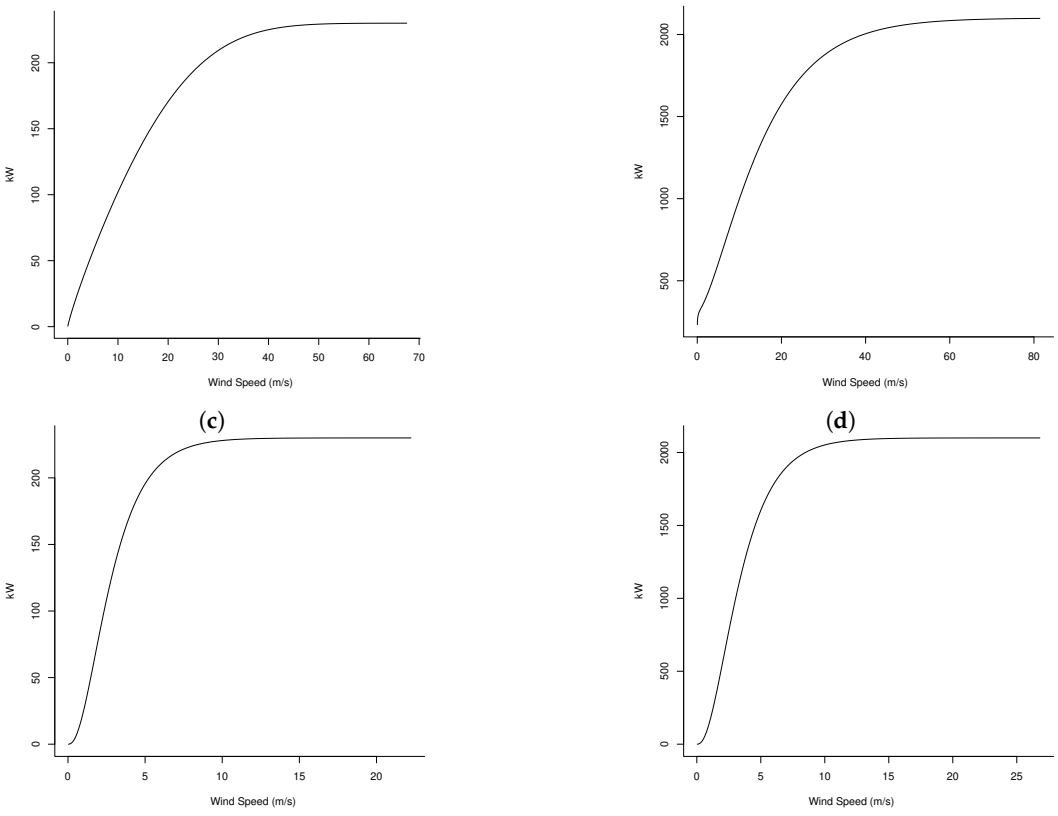

Figure 9. Power curves for the considered wind turbines at the three stations. (**a**) Power curve for the Clínica station–Endurance X33. (**b**) Power curve for the Clínica station–SuzlonS88/2100. (**c**) Power curve for the Anapra station–Endurance X33. (**d**) Power curve for the Anapra station–SuzlonS88/2100. (**e**) Power curve for the IIT station–Endurance X33. (**f**) Power curve for the IIT station–SuzlonS88/2100.

5. Conclusions

In this paper, an analysis of the wind energy potential was performed in the area of Ciudad Juárez, México. The proposed analysis considered the first model and collected wind speed data from three meteorological stations by taking into account different distributions that have been proposed in the literature as adequate options. These distributions included the Weibull distribution and some variations, such as the exponentiated Weibull and inverse Weibull. Mixture distributions have also been deemed an important option when dealing with wind speed data.

The mixture distributions along with the exponentiated Weibull for the three stations that best-fitted the data according to information criteria were found. As the exponentiated Weibull distribution has not been considered in the literature to describe wind speed data, it may be an important option for further analysis of this type of data. In this sense, these best-fitted distributions were used to characterize PCs under the consideration of two wind turbines. Specifically, the PCs were defined based on the best-fitting CDFs and the power profile of the considered turbines. These PCs allow us to obtain the perspective of the energy production potential for the wind speed of the region.

Furthermore, based on these PCs, the annual energy production was estimated. According to the reported results, energy production is consistent in the three locations; for the Clínica station, more energy can be produced (48.2 MWh). This is consistent with the collected wind speed data, as the higher mean wind speed was collected from this station. To complement the analysis, the log law was considered to extrapolate the collected wind speed to assess the energy production by considering wind turbines with greater heights. Two other prospective wind turbines were studied by defining their respective PCs

and energy production based on the proposed method. This provides an opportunity to consider further options for energy generation in different locations of the studied region.

The results reported in this study complement the efforts of assessing the wind energy potential of any region. In addition to the proposed models, other approaches can be considered for further analysis. Stochastic approaches and machine learning techniques can be considered when modeling wind speed data. However, this will require the proposal of different approaches for the characterization of PCs. On the other hand, four specific wind turbines may be considered to illustrate the proposed approach. However, a thorough technical analysis may be required to determine adequate wind turbines that can be considered for energy production in the region of interest. Furthermore, other factors should be analyzed that influence the adoption of wind energy production strategies, such as geographical regions, financial investment, governmental initiatives, and fossil fuel supply disruption [57].

Author Contributions: Conceptualization, C.A.H.-M. and L.A.R.-P.; methodology, C.A.H.-M. and L.A.R.-P.; software, L.A.R.-P.; validation, L.A.R.-P.; formal analysis, C.A.H.-M. and L.A.R.-P.; investigation, C.A.H.-M., L.A.R.-P., F.A.V.-G., and J.I.H.-H.; resources, F.A.V.-G.; data curation, C.A.H.-M., L.A.R.-P., I.J.C.P.-O., F.A.V.-G. and J.I.H.-H.; writing—original draft preparation, C.A.H.-M., L.A.R.-P. and I.J.C.P.-O.; writing—review and editing, C.A.H.-M., L.A.R.-P. and I.J.C.P.-O.; visualization, I.J.C.P.-O. and L.C.M.-G.; funding acquisition, L.A.R.-P., I.J.C.P.-O., F.A.V.-G., J.I.H.-H. and L.C.M.-G. All authors have read and agreed to the published version of the manuscript.

Funding: The APC was partly funded by the Universidad Autónoma de Ciudad Juárez.

Institutional Review Board Statement: Not applicable.

Informed Consent Statement: Not applicable.

Data Availability Statement: The data presented in this study are openly available in the Laboratorio de Climatología y Calidad del Aire at https://erecursos.uacj.mx/communities/b27494f3-ef56-4f2b-9b58-12db83e20176 (accessed on 1 December 2023).

Conflicts of Interest: The authors declare no conflicts of interest.

References

1. Pishgar-Komleh, S.; Keyhani, A.; Sefeedpari, P. Wind speed and power density analysis based on Weibull and Rayleigh distributions (a case study: Firouzkooh county of Iran). *Renew. Sustain. Energy Rev.* **2015**, *42*, 313–322. [CrossRef]
2. Song, J.; Wang, J.; Lu, H. A novel combined model based on advanced optimization algorithm for short-term wind speed forecasting. *Appl. Energy* **2018**, *215*, 643–658. [CrossRef]
3. Khosravi, A.; Koury, R.; Machado, L.; Pabon, J. Energy, exergy and economic analysis of a hybrid renewable energy with hydrogen storage system. *Energy* **2018**, *148*, 1087–1102. [CrossRef]
4. Zuluaga, C.D.; Álvarez, M.A.; Giraldo, E. Short-term wind speed prediction based on robust Kalman filtering: An experimental comparison. *Appl. Energy* **2015**, *156*, 321–330. [CrossRef]
5. Li, D.; Zhang, Z.; Zhou, X.; Zhang, Z.; Yang, X. Cross-wind dynamic response of concrete-filled double-skin wind turbine towers: Theoretical modelling and experimental investigation. *J. Vib. Control* **2023**, *30*, 2881–2893. [CrossRef]
6. Li, D.; Fang, S.; Sun, C.; Zhang, Z.; Lai, Z. Passive structural control for wind turbine towers using a novel dual-track nonlinear energy sink. *J. Vib. Control.* **2024**. [CrossRef]
7. Brano, V.L.; Orioli, A.; Ciulla, G.; Culotta, S. Quality of wind speed fitting distributions for the urban area of Palermo, Italy. *Renew. Energy* **2011**, *36*, 1026–1039. [CrossRef]
8. Li, G.; Shi, J. Application of Bayesian model averaging in modeling long-term wind speed distributions. *Renew. Energy* **2010**, *35*, 1192–1202. [CrossRef]
9. Morgan, E.C.; Lackner, M.; Vogel, R.M.; Baise, L.G. Probability distributions for offshore wind speeds. *Energy Convers. Manag.* **2011**, *52*, 15–26. [CrossRef]
10. Ouarda, T.B.; Charron, C.; Shin, J.Y.; Marpu, P.R.; Al-Mandoos, A.H.; Al-Tamimi, M.H.; Ghedira, H.; Al Hosary, T. Probability distributions of wind speed in the UAE. *Energy Convers. Manag.* **2015**, *93*, 414–434. [CrossRef]
11. Wais, P. A review of Weibull functions in wind sector. *Renew. Sustain. Energy Rev.* **2017**, *70*, 1099–1107. [CrossRef]
12. Zhou, Y.; Wu, W.; Liu, G. Assessment of onshore wind energy resource and wind-generated electricity potential in Jiangsu, China. *Energy Procedia* **2011**, *5*, 418–422. [CrossRef]
13. Tuller, S.E.; Brett, A.C. The goodness of fit of the Weibull and Rayleigh distributions to the distributions of observed wind speeds in a topographically diverse area. *J. Climatol.* **1985**, *5*, 79–94. [CrossRef]

14. Mohammadi, K.; Alavi, O.; Mostafaeipour, A.; Goudarzi, N.; Jalilvand, M. Assessing different parameters estimation methods of Weibull distribution to compute wind power density. *Energy Convers. Manag.* **2016**, *108*, 322–335. [CrossRef]
15. Carta, J.A.; Ramirez, P.; Velazquez, S. A review of wind speed probability distributions used in wind energy analysis: Case studies in the Canary Islands. *Renew. Sustain. Energy Rev.* **2009**, *13*, 933–955. [CrossRef]
16. Genc, A.; Erisoglu, M.; Pekgor, A.; Oturanc, G.; Hepbasli, A.; Ulgen, K. Estimation of wind power potential using Weibull distribution. *Energy Sources* **2005**, *27*, 809–822. [CrossRef]
17. Zheng, H.; Huang, W.; Zhao, J.; Liu, J.; Zhang, Y.; Shi, Z.; Zhang, C. A novel falling model for wind speed probability distribution of wind farms. *Renew. Energy* **2022**, *184*, 91–99. [CrossRef]
18. Wais, P. Two and three-parameter Weibull distribution in available wind power analysis. *Renew. Energy* **2017**, *103*, 15–29. [CrossRef]
19. Wan, J.; Zheng, F.; Luan, H.; Tian, Y.; Li, L.; Ma, Z.; Xu, Z.; Li, Y. Assessment of wind energy resources in the urat area using optimized weibull distribution. *Sustain. Energy Technol. Assessments* **2021**, *47*, 101351. [CrossRef]
20. Saeed, M.A.; Ahmed, Z.; Hussain, S.; Zhang, W. Wind resource assessment and economic analysis for wind energy development in Pakistan. *Sustain. Energy Technol. Assessments* **2021**, *44*, 101068. [CrossRef]
21. Akgül, F.G.; Şenoğlu, B.; Arslan, T. An alternative distribution to Weibull for modeling the wind speed data: Inverse Weibull distribution. *Energy Convers. Manag.* **2016**, *114*, 234–240. [CrossRef]
22. Chang, T.P. Performance comparison of six numerical methods in estimating Weibull parameters for wind energy application. *Appl. Energy* **2011**, *88*, 272–282. [CrossRef]
23. Shata, A.A.; Hanitsch, R. Evaluation of wind energy potential and electricity generation on the coast of Mediterranean Sea in Egypt. *Renew. Energy* **2006**, *31*, 1183–1202. [CrossRef]
24. Han, K.; Choi, J.; Kim, C. Comparison of statistical post-processing methods for probabilistic wind speed forecasting. *Asia-Pac. J. Atmos. Sci.* **2018**, *54*, 91–101. [CrossRef]
25. Liu, F.J.; Chang, T.P. Validity analysis of maximum entropy distribution based on different moment constraints for wind energy assessment. *Energy* **2011**, *36*, 1820–1826. [CrossRef]
26. Rajabi, M.; Modarres, R. Extreme value frequency analysis of wind data from Isfahan, Iran. *J. Wind Eng. Ind. Aerodyn.* **2008**, *96*, 78–82. [CrossRef]
27. Ouarda, T.B.; Charron, C. On the mixture of wind speed distribution in a Nordic region. *Energy Convers. Manag.* **2018**, *174*, 33–44. [CrossRef]
28. Kollu, R.; Rayapudi, S.R.; Narasimham, S.; Pakkurthi, K.M. Mixture probability distribution functions to model wind speed distributions. *Int. J. Energy Environ. Eng.* **2012**, *3*, 27. [CrossRef]
29. Carta, J.; Ramirez, P. Analysis of two-component mixture Weibull statistics for estimation of wind speed distributions. *Renew. Energy* **2007**, *32*, 518–531. [CrossRef]
30. Wang, J.; Hu, J.; Ma, K. Wind speed probability distribution estimation and wind energy assessment. *Renew. Sustain. Energy Rev.* **2016**, *60*, 881–899. [CrossRef]
31. Asghar, A.B.; Liu, X. Estimation of wind speed probability distribution and wind energy potential using adaptive neuro-fuzzy methodology. *Neurocomputing* **2018**, *287*, 58–67. [CrossRef]
32. Zhang, Y.; Pan, G.; Zhao, Y.; Li, Q.; Wang, F. Short-term wind speed interval prediction based on artificial intelligence methods and error probability distribution. *Energy Convers. Manag.* **2020**, *224*, 113346. [CrossRef]
33. Miao, S.; Gu, Y.; Li, D.; Li, H. Determining suitable region wind speed probability distribution using optimal score-radar map. *Energy Convers. Manag.* **2019**, *183*, 590–603. [CrossRef]
34. Fadare, D. The application of artificial neural networks to mapping of wind speed profile for energy application in Nigeria. *Appl. Energy* **2010**, *87*, 934–942. [CrossRef]
35. Ouarda, T.B.; Charron, C.; Chebana, F. Review of criteria for the selection of probability distributions for wind speed data and introduction of the moment and L-moment ratio diagram methods, with a case study. *Energy Convers. Manag.* **2016**, *124*, 247–265. [CrossRef]
36. Jónsdóttir, G.M.; Milano, F. Data-based continuous wind speed models with arbitrary probability distribution and autocorrelation. *Renew. Energy* **2019**, *143*, 368–376. [CrossRef]
37. Calero, R.; Carta, J.A. Action plan for wind energy development in the Canary Islands. *Energy Policy* **2004**, *32*, 1185–1197. [CrossRef]
38. Canavos, G.C. *Applied Probability and Statistical Methods*; Little, Brown: Boston, MA, USA, 1984.
39. Akaike, H. A new look at the statistical model identification. *IEEE Trans. Autom. Control* **1974**, *19*, 716–723. [CrossRef]
40. Ochoa, G.V.; Alvarez, J.N.; Chamorro, M.V. Data set on wind speed, wind direction and wind probability distributions in Puerto Bolivar-Colombia. *Data Brief* **2019**, *27*, 104753. [CrossRef]
41. Chen, H.; Anfinsen, S.N.; Birkelund, Y.; Yuan, F. Probability distributions for wind speed volatility characteristics: A case study of Northern Norway. *Energy Rep.* **2021**, *7*, 248–255. [CrossRef]
42. Li, D.; Miao, S. Fitting the wind speed probability distribution with Maxwell and power Maxwell distributions: A case study of North Dakota sites. *Sustain. Energy Technol. Assessments* **2021**, *47*, 101446. [CrossRef]
43. Bokde, N.; Feijóo, A.; Villanueva, D. Wind turbine power curves based on the weibull cumulative distribution function. *Appl. Sci.* **2018**, *8*, 1757. [CrossRef]

44. Lydia, M.; Selvakumar, A.I.; Kumar, S.S.; Kumar, G.E.P. Advanced algorithms for wind turbine power curve modeling. *IEEE Trans. Sustain. Energy* **2013**, *4*, 827–835. [CrossRef]
45. Kusiak, A.; Zheng, H.; Song, Z. On-line monitoring of power curves. *Renew. Energy* **2009**, *34*, 1487–1493. [CrossRef]
46. Zafirakis, D.; Paliatsos, A.; Kaldellis, J. Energy Yield of Contemporary Wind Turbines. In *Comprehensive Renewable Energy*; Elsevier: Amsterdam, The Netherlands, 2012; pp. 113–168. [CrossRef]
47. de Mexico, G. Servicio Meteorológico Nacional. Available online: https://smn.conagua.gob.mx/es/ (accessed on 1 January 2022).
48. Windfinder. Predicciones de viento, mapa de viento, velocidad del viento y observaciones meteorologicas. Available online: https://www.windfinder.com/#3/39.5000/-98.3500/spot (accessed on 1 January 2023).
49. de Ciudad Juárez, U.A. Laboratorio de Climatologia y Calidad del aire. Available online: https://erecursos.uacj.mx/communities/b27494f3-ef56-4f2b-9b58-12db83e20176 (accessed on 1 December 2023).
50. Pal, M.; Ali, M.M.; Woo, J. Exponentiated weibull distribution. *Statistica* **2006**, *66*, 139–147. [CrossRef]
51. Folks, J.L.; Chhikara, R.S. The inverse Gaussian distribution and its statistical application—A review. *J. R. Stat. Soc. Ser. B (Methodological)* **1978**, *40*, 263–275. [CrossRef]
52. Khamees, A.K.; Abdelaziz, A.Y.; Ali, Z.M.; Alharthi, M.M.; Ghoneim, S.S.; Eskaros, M.R.; Attia, M.A. Mixture probability distribution functions using novel metaheuristic method in wind speed modeling. *Ain Shams Eng. J.* **2022**, *13*, 101613. [CrossRef]
53. Delignette-Muller, M.L.; Dutang, C. fitdistrplus: An R package for fitting distributions. *J. Stat. Softw.* **2015**, *64*, 1–34. [CrossRef]
54. Shalizi, C. F-Tests, R^2, and Other Distractions, 2015. Carnegie Mellon Institute. Available online: https://www.stat.cmu.edu/~cshalizi/mreg/15/lectures/10/lecture-10.pdf (accessed on 1 January 2023).
55. Carrillo, C.; Montaño, A.O.; Cidrás, J.; Díaz-Dorado, E. Review of power curve modelling for wind turbines. *Renew. Sustain. Energy Rev.* **2013**, *21*, 572–581. [CrossRef]
56. Manwell, J.F.; McGowan, J.G.; Rogers, A.L. *Wind Energy Explained: Theory, Design and Application*; John Wiley & Sons: Hoboken, NJ, USA, 2010.
57. Debnath, B.; Shakur, M.S.; Siraj, M.T.; Bari, A.M.; Islam, A.R.M.T. Analyzing the factors influencing the wind energy adoption in Bangladesh: A pathway to sustainability for emerging economies. *Energy Strategy Rev.* **2023**, *50*, 101265. [CrossRef]